Scaling properties of conduction velocity in heterogeneous excitable media

T. K. Shajahan, Bartłomiej Borek, Alvin Shrier, and Leon Glass
Department of Physiology, McGill University, Montreal, Canada
(Received 9 September 2010; revised manuscript received 29 June 2011; published 20 October 2011)

Waves of excitation through excitable media, such as cardiac tissue, can propagate as plane waves or break up to form reentrant spiral waves. In diseased hearts reentrant waves can be associated with fatal cardiac arrhythmias. In this paper we investigate the conditions that lead to wave break, reentry, and propagation failure in mathematical models of heterogeneous excitable media. Two types of heterogeneities are considered: *sinks* are regions in space in which the voltage is fixed at its rest value, and *breaks* are nonconducting regions with no-flux boundary conditions. We find that randomly distributed heterogeneities in the medium have a decremental effect on the velocity, and above a critical density of such heterogeneities the conduction fails. Using numerical and analytical methods we derive the general relationship among the conduction velocity, density of heterogeneities, diffusion coefficient, and the rise time of the excitation in both two and three dimensions. This work helps us understand the factors leading to reduced propagation velocity and the formation of spiral waves in heterogeneous excitable media.

DOI: 10.1103/PhysRevE.84.046208 PACS number(s): 89.75.Kd, 87.19.Hh, 87.18.Hf

I. INTRODUCTION

Analysis of wave propagation through spatially heterogeneous media is a classic problem in physics [1,2]. Here we consider nonlinear excitable media, such as nerve, heart, or the Belousov-Zhabotinsky (BZ) reaction in which a sufficiently large perturbation from the equilibrium state can lead to propagation of a wave. A typical behavior in an excitable medium is that a wave once started will propagate to the end of the medium or will annihilate if it collides with a wave coming from another direction. However, even in a homogeneous excitable medium, the dynamics can be unstable to small perturbations, leading to transient dynamics in the system that in turn result in wave break and spiral waves [3–5]. A further complication arises in natural and experimental excitable systems, which necessarily contain heterogeneities that lead to a variety of experimentally observed wave patterns including rotating spiral waves. Examples include heterogeneities in the form of water-in-oil microemulsions [6,7] and experimentally generated catalyst patches in the Belousov-Zhabotinsky reaction [8], irregularities in catalytic surfaces [9–11], and variability in the spatial structure in cardiac tissue and tissue culture [12–18]. Figure 1 shows an example of such spiral waves in a monolayer tissue culture from embryonic chick heart cells. The wave of calcium activity here interacts with the heterogeneities in the culture, resulting in wave break and reentry. Similarly, pathologically induced heterogeneities in the whole heart, such as may be induced by fibrosis of the heart, may lead to reentrant activation patterns that are associated with serious abnormal cardiac rhythms [16,17,19].

As a consequence of the underlying theoretical challenges and their practical importance, there are many studies of the role of heterogeneities in modulating cardiac conduction. These studies analyze the roles of both localized [18,20–25] and randomly distributed heterogeneities [12–17,26–28]. While large localized heterogeneities often act as anchoring sites for spiral waves of excitation, smaller, randomly dispersed heterogeneities have more subtle effects on the dynamics. The effects depend on the excitability of the medium, the properties of the medium in the absence of heterogeneities, and the types of heterogeneities. We will consider two different types of heterogeneities. *Breaks* are nonconducting regions with no-flux boundary conditions that represent discontinuities resulting from tissue damage and collagen deposition [26,27], while *sinks* are regions in space in which the voltage is fixed at its rest value, similar to fibroblast cells which are coupled to excitable myocytes [15,16,28]. As the density of random heterogeneities increases, the conduction velocity typically decreases. This can have contrasting effects depending on the underlying properties of the medium. If the medium normally conducts plane waves without breaking up, then as the density of heterogeneities increases or if the excitability of the medium decreases, the propagation slows and eventually becomes unstable, leading to rotating spiral waves [13,14,28]. In contrast, for excitable media in which spiral wave propagation is unstable, an increase of heterogeneity can lead to a subsequent slowing of the propagating wave and paradoxical stabilization of the propagation [26,27,29].

Recent work has focused on understanding the decrease of propagation velocity as a function of the density of heterogeneities. Steinberg *et al.* proposed a dimensionless number to characterize media at the point where plane waves break up [28]. Bär and co-workers developed an effective medium theory in which effective diffusion coefficients and reaction rates describe the decrease of conduction velocity with heterogeneity density [9–11].

In this paper we extend these earlier studies to show the general relationship among conduction velocity, heterogeneity, and cell-cell coupling in model cardiac systems with breaks and sinks. Specifically, we look at the conduction velocity of plane waves and study how the density of heterogeneities and the coupling between cells affect conduction velocity. Using numerical and analytical methods we propose a functional form for the relationship among the conduction velocity, coupling, and the density of the heterogeneities.

This paper is organized as follows. In Sec. II we describe the mathematical models used in this study. Section III contains

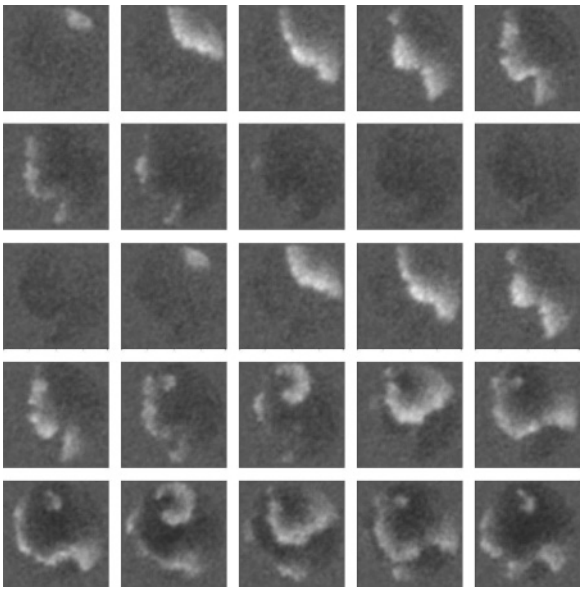

FIG. 1. Snapshots of wave propagation in a cardiac monolayer culture. The images show a calcium wave in a monolayer culture of chick embryonic heart cells. The diameter of the monolayer is 1 cm, and the brighter areas indicate high intracellular calcium concentration. The panels are 0.25 s apart. A wave starting from top right corner of the culture propagates through the heterogeneous medium to the left boundary. But the second wave is unable to maintain its planar wave front, and the breaks lead to reentry.

numerical results of the velocity–heterogeneity density relationship in these models. In Sec. IV we present a theoretical model for a single sink, and Sec. V contains a discussion of the results.

II. MODELS OF EXCITABLE MEDIA

In this work we determine the velocity of wave propagation for two different models of excitable media. Because our primary focus is application to cardiac tissue, we assume parameter values consistent with cardiac conduction.

A. Cellular automata

We study the effects of heterogeneities in a variant of the Greenberg-Hastings (GH) cellular automata model [13,30]. Each site (ij) in the medium at time t is assigned an integer state, $u_{ij}(t)$, falling between 0 and $\mathscr{E}+\mathscr{R}$, where 0 is the rest state, $1,2,\ldots,\mathscr{E}$, are excited states, and $\mathscr{E}+1,\mathscr{E}+2,\ldots,\mathscr{E}+\mathscr{R}$ are refractory states. In this work, we use $\mathscr{E}=6$ and $\mathscr{R}=7$. We introduce spatial heterogeneity by assigning coordinates $(i+\epsilon_i,\ j+\epsilon_j)$, where ϵ_i and ϵ_j are uniformly distributed in the interval $[-0.5,0.5]$ [13]. To simplify theoretical calculations, the distance between two sites (i,j) and (k,l) is represented by $D[ki]$ and $D[lj]$, where $D[ki]=(|(k+\epsilon_k)-(i+\epsilon_i)|$. With this distance metric two sites (i,j) and (k,l) are within a radius r if $D[ki]\&D[lj]<r$, i.e., these points lie within a square of side r. Each cell is also assigned a random weight, S_{ij}, for the cell's influence on its neighbors. S_{ij} is assigned values from 0.5 to 1.5 randomly. A certain fraction of the sites, ϕ, are assumed to be in a state 0 for all times. These sites correspond to inexcitable heterogeneities. For the other cells the transition rules are as follows. If $1\leqslant u_{ij}(t)<\mathscr{E}+\mathscr{R}$, then $u_{ij}(t+1)=u_{ij}(t)+1$ and if $u_{ij}(t)=\mathscr{E}+\mathscr{R}$, $u_{ij}(t+1)=0$. If $u_{ij}(t)=0$, then $u_{ij}=1$ if $\frac{\sum_{D[ki]\&D[lj]<r;0<u_{kl}\leqslant\mathscr{E}}S_{kl}}{\sum_{D[ki]\&D[lj]\langle r;u_{mn}=0 or u_{mn})\mathscr{E}}S_{mn}}>\theta$. This means that in order for a cell to be excited at time $t+1$ the ratio of excited cells to the cells that are in the resting state $(u=0)$ in a neighborhood of radius r at time t must be greater than θ. We assume cells are separated by a distance of 0.01 cm and that each time step is 1 ms.

B. FitzHugh-Nagumo equations

The FitzHugh-Nagumo (FHN) equations are

$$\begin{aligned}\frac{\partial e}{\partial t}&=D\nabla^2 e+e(e-\alpha)(1-e)-g+I(r),\\ \frac{\partial g}{\partial t}&=\epsilon(\beta e-g),\end{aligned}\tag{1}$$

where D is the diffusion coefficient and $I(r)$ is the applied perturbation at position r. The fast variable e is like a dimensionless transmembrane potential scaled to unity. e varies between 0 and $e_{\max}=1$. The slow variable g controls the refractory period. We assume $\alpha=0.02$, $\epsilon=0.01$, and $\beta=0.5$, with D varying in the range 0.5–5.0 cm^2/s.

We solve these equations numerically in two dimensions in a 200×200 grid and in three dimensions in a $200\times200\times200$ grid. We use forward Euler integration with space step $\delta x=0.01$ and time step δt from 0.001 to 0.01. We take the spatial unit to be 1 cm and time unit to be 1 ms. With this choice of space and time units, the velocity varies between 14 and 40 cm/s for the range of D we consider.

In the FHN model, we define *sinks* by clamping cells at random locations to their rest state $(e=0,g=0)$ (i.e., Dirichlet boundary conditions) and *breaks* by using Neumann boundary conditions at randomly located heterogeneities. To characterize and analyze the effects of heterogeneities, we measure conduction velocity v of the waves as a function of the density of heterogeneous sites, ρ (measured in number of sites per cm^2). v is calculated by measuring the activation times across a line perpendicular to the direction of propagation, at $(N/4)$th and $(3N/4)$th sites in the medium, where N is the size of the simulation domain. This gives the time taken for the wave to travel $N/2$ sites. We take the median of the resultant velocity values. For the simulations in the FHN model, ten different realizations of heterogeneities were used, and the mean across the distributions is presented. The standard error of the mean velocity is less than 2% in the regime where the conduction velocity depends linearly on ρ for both the sinks and breaks.

III. VELOCITY–HETEROGENEITY DENSITY RELATIONSHIP

A. Cellular automata

In the discrete model, the velocity is the average distance an excitation progresses in one iteration. We assume that the time interval between iterations is Δt. Following Bub *et al.* [13] we can estimate the velocity of the plane wave in the GH model as follows. Assume the wave front is smooth. A cell at a distance δ away from this wave front, where $\delta<r$, will have

$2r(r-\delta)$ excited cells in its neighborhood. Hence the ratio of excited cells to nonexcited cells (i.e., all cells in the rest state) is $(r-\delta)/(r+\delta)$. If δ is the distance an excitation can travel in one iteration this ratio would be equal to θ. Hence the velocity in terms of r and θ is given by

$$v_0^{GH} = \delta/\Delta t = \frac{r(1-\theta)}{\Delta t(1+\theta)}. \tag{2}$$

This gives us an upper estimate of the velocity, v_0^{GH}, of the plane wave in this model.

We now extend this result to include the effects of nonexcitable cells. Again consider a cell at a distance δ away from the wave front. The area in the neighborhood of the cell that is excited is $2r(r-\delta)(1-\phi)$, where ϕ is the fraction of nonexcitable cells. Similarly, the area that is not excited is $2r(r+\delta)+2r(r-\delta)\phi$. For the cell to be excited their ratio has to be greater than θ. Hence the velocity is

$$v^{GH} = \delta/\Delta t = \frac{r[1-\theta-(1+\theta)\phi]}{\Delta t(1+\theta)(1-\phi)}. \tag{3}$$

By using Eq. (2), the result can be rewritten as

$$v^{GH} = v_0^{GH}\left(\frac{1-\phi\left(\frac{1+\theta}{1-\theta}\right)}{1-\phi}\right). \tag{4}$$

Although this result is for a highly oversimplified model for heterogeneities in excitable media, as we show below, the dependence of the velocity on heterogeneity density is similar to the dependence in the more realistic models.

We simulate the GH model in two dimensions with 200×200 points. A plane wave was initiated at one side of the simulation domain. The velocity is calculated from the minimum time required for the wave to excite any cell at the other end of the domain. Figure 2(a) shows the velocity thus calculated with $\theta = 0.35$ and for r values of 0.025, 0.03, 0.035, 0.04, and 0.045 cm. In Fig. 2(b) we show the normalized velocity from Eq. (4) superimposed on the theoretical curve. There is a good agreement between the numerical simulations and the theoretical estimate.

B. FHN model

1. Breaks

Previous studies [9,14,31] of heterogeneous excitable media with diffuse heterogeneities have largely focused on

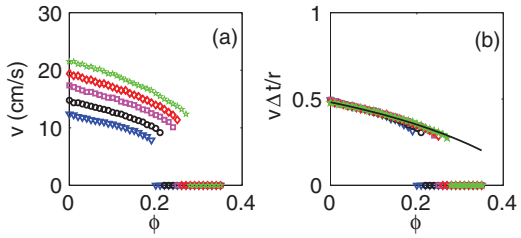

FIG. 2. (Color online) (a) Conduction velocity in the Greenberg-Hastings model for r values 0.025 (triangles), 0.03 (circles), 0.035 (squares), 0.04 (diamonds), and 0.045 (stars) as we vary the fraction of heterogeneities ϕ. (b) $v\Delta t/r$ plotted against ϕ. The solid line is the theoretically calculated value of $v^{GH}\Delta t/r$ from Eq. (3) for $\theta = 0.35$.

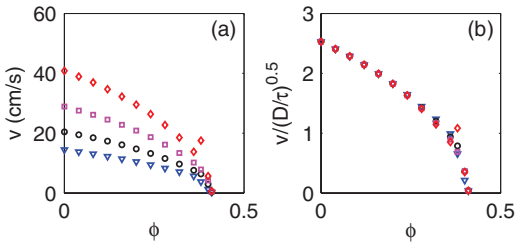

FIG. 3. (Color online) (a) Conduction velocity v as a function of fraction of breaks, ϕ, for $D = 0.5$ (triangles), 1.0 (open circles), 2.0 (squares), and 4.0 (diamonds) cm^2/s in the FHN model. (b) $v/\sqrt{D/\tau}$ plotted against ϕ.

break heterogeneities. When there are many small break-heterogeneities randomly distributed in the system, for low density of breaks, Tusscher and co-workers [29,31] found that the conduction velocity of the waves of excitation decreases linearly. We extend these studies with many breaks and look at how coupling in the medium affects velocity. According to Luther's law [32,33] the propagation velocity of plane waves in a homogeneous medium, v_0, is given by

$$v_0 = k\sqrt{D/\tau}, \tag{5}$$

where k is a constant and τ is the rise time of excitation. In a heterogeneous medium, when $\phi < 0.40$, conduction velocity decreases linearly with ϕ [Fig. 3(a)], where $\phi = \rho l_b^2$ represents the fraction of breaks in the medium and l_b^2 the area of a break. The slope of v versus ϕ curve depends only on v_0, as shown in Fig. 3(b), where $v/\sqrt{D/\tau}$ is plotted as a function of ϕ. It is easy to deduce from this figure that the conduction velocity in the linear regime decreases as

$$v = k\sqrt{D/\tau}(1-c\phi), \tag{6}$$

where c is a constant. Further increase in ϕ leads to conduction failure when $\phi = \phi_c \simeq 0.41$, which corresponds to a density of 4100 breaks/cm^2, independent of D. The value of $\phi_c \simeq 0.41$ for conduction failure is the same as the site percolation threshold for a square lattice [34–36]. This implies that the wave can propagate between breaks as long as it can find a connected path in the medium. Similar results were obtained in the studies of the BZ reaction with random fluctuations in excitability [37]. Here when the fraction of the nonexcitable region exceeds the percolation threshold, the conduction fails, irrespective of the dynamics in the medium. Hence we conclude that the breaks only disconnect the propagation pathway and do not otherwise modify the properties of propagation.

The simulations in Fig. 3 are done with breaks of size δx^2. If we use breaks of size $4\delta x^2$ we find a linear decline of velocity Eq. (6) and conduction failure at $\phi_c \simeq 0.44$. For breaks of $9\delta x^2$, $\phi_c \simeq 0.55$. The dependence of the conduction on the size and the shape of the breaks requires further study.

2. Sinks

Earlier studies on the dependence of conduction velocity in an excitable medium with sink heterogeneities described a linear decrease in velocity as a function of the density of sinks [28]. The basic idea was to develop theoretical insight

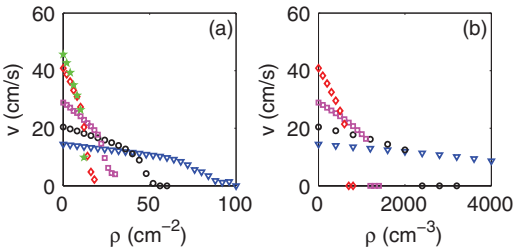

FIG. 4. (Color online) (a) Conduction velocity v in the two-dimensional FHN model as a function of density of sinks, ρ, for $D = 0.5$ (triangles), 1.0 (circles), 2.0 (squares), 4.0 (diamonds), and 5.0 (stars) cm^2/s. (b) v in the three-dimensional FHN model as a function of ρ. Symbols have the same meaning as in (a).

into this finding using dimensional arguments. The current work was motivated by an attempt to critically examine and extend these earlier studies. However, numerical studies carried out in the course of this work, both in two dimensions and three dimensions, over broader parameter ranges than those initially studied [28] showed discrepancies between the proposed scaling relationships and the computed values.

To study the formation of reentrant waves in a heterogeneous medium we initiate plane waves in the two-dimensional FHN model. When the medium is homogeneous the velocity, v_0, is given by Eq. (5). In a heterogeneous medium the velocity decreases from v_0. Figure 4(a) shows the velocity as a function of the density of sinks (ρ) for D between 0.5 to 5.0 cm^2/s. For example, consider a medium with $D = 0.5$ cm^2/s. When the heterogeneities are very sparse in the medium ($\rho < 36$ cm^{-2}), the wave travels as a roughened plane wave, and the velocity decreases approximately linearly. For $\rho \sim 36$–58 the plane wave breaks in several places, but it soon reforms, generating a quasi-planar wave front. With a still higher density, the wave breaks up, forming curved wave fronts leading to sustained reentrant waves and spatiotemporally irregular patterns of activation in the medium (Fig. 5). This region is represented by a steeper, nonlinear change in velocity with ρ as in Fig. 4(a). Here, in addition to the effects of the heterogeneities, the convex wave-front curvature also contributes to a slowing of the conduction velocity [38]. With an even higher density of sinks ($\rho > 100$ cm^{-2}) the wave is unable to propagate through the medium, and the conduction fails at a critical density, $\rho = \rho_c$.

Similar dynamics are also observed in the three-dimensional FHN model. In Fig. 6 we show snapshots of propagation in the three-dimensional FHN model for $\rho = 200$ cm^{-3} and $\rho = 1000$ cm^{-3}. At even higher densities there are more wave breaks in the medium. In Fig. 4(b) we show the decline of propagation velocity with heterogeneity density for D from 0.5 to 4.0 cm^2/s. As in two dimensions, the velocity decreases linearly for smaller ρ and eventually the conduction fails at a critical density ρ_c.

The slope of the linear regime and the critical density depends on the diffusion coefficient in the medium, as seen in Fig. 4. In our simulations, the velocity decreases at a rate $\propto v_0\rho(D)^\gamma$ and conduction fails at constant $\rho(D)^\gamma$, where $\gamma \simeq 0.77$ in two dimensions and $\gamma \simeq 1.01$ in three dimensions. In our previous paper [28] we found that the conduction fails for constant values of $\sqrt{\rho D}$. To further explore the change

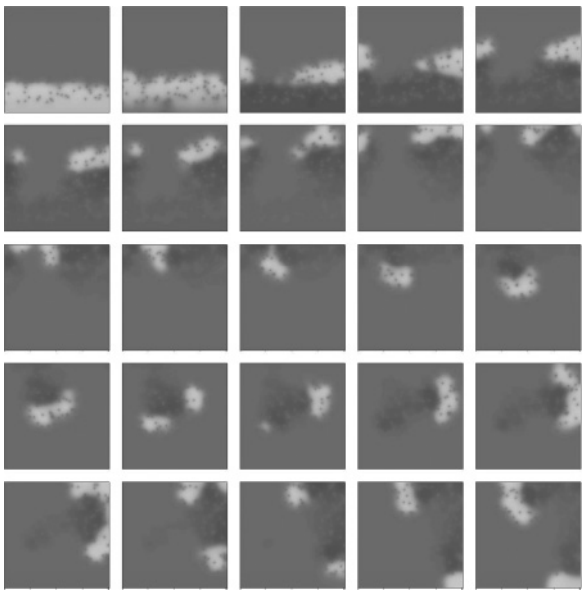

FIG. 5. Snapshots of wave propagation in the FitzHugh-Nagumo model [Eq. (1), with $D = 0.6$ cm^2/s and $\rho = 60$/cm^2]. We initiate a plane wave from the lower boundary of the simulation domain which breaks up and forms reentrant circuits. The brighter areas represent regions with high activation. The panels are separated by 5 ms.

in conduction velocity in the presence of sink heterogeneities, we analyze the change in velocity because of a single sink and develop an analytical model for it. This model can help us understand how wave propagation is modified in the presence of many such sinks randomly distributed in the medium.

IV. EFFECT OF A SINGLE SINK ON PROPAGATION

A. Numerical study

To study how a single sink modifies propagation in an excitable medium, we analyze properties of propagation in a simulation domain with 200 × 200 grid points. The sink is placed at $(x = 100, y = y_{\text{sink}})$, where y_{sink} is varied from 60 to 120. In this medium we measure velocity by measuring the activation times at the 50th and 150th sites along the y direction. In the absence of the sink the wave arrives simultaneously at all points along the line at $y = 150$. But when there is a sink present, the activation will be delayed near the sink position ($x = 100$). We plot this delay in Fig. 7(a) as a function of x, for $y_{\text{sink}} = 120, 80$, and 60 when $D = 1.0$ cm^2/s.

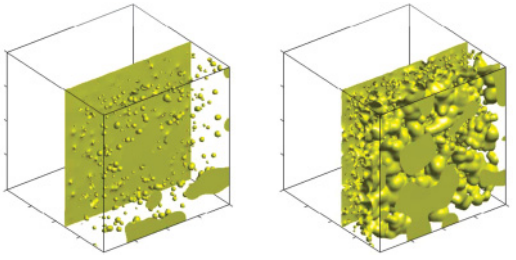

FIG. 6. (Color online) Isosurface plots of wave propagation for the three-dimensional FHN model with heterogeneities when $D = 0.7$ cm^2/s for $\rho = 200$ cm^{-3} (left) and for $\rho = 1000$ cm^{-3} (right).

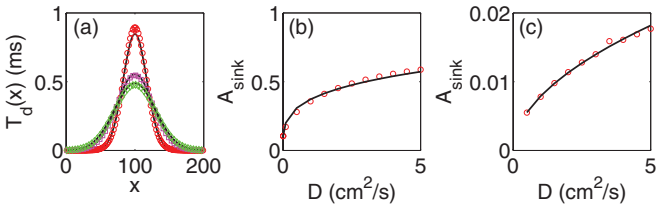

FIG. 7. (Color online) (a) Change in crossing time $[T_d(x)]$ along the x direction because of a single sink located at $x = 100$ grid points and $y = 120$ (circles), 80 (squares), and 60 (diamonds) for $D = 1.0$ cm^2/s. The solid lines are the solutions of the one-dimensional diffusion equation with an instantaneous point source of amplitude $A_{\text{sink}} = 0.36$ ms cm located at $x = 100$. (b) A_{sink} plotted as a function of D (open circles). The solid line is the best-fitting curve $A_{\text{sink}} = 0.37D^{0.27}$. (c) In three-dimensional media, $T_d(x)$ behaves like solutions of the two-dimensional diffusion equation from a point source of strength A_{sink} ms cm^2. A_{sink} in three dimensions is plotted here (open circles) as a function of D. The solid line is the best-fitting curve $A_{\text{sink}} = 0.0079D^{0.52}$.

The profile of activation times is narrower when $y_{\text{sink}} = 120$ and is broader when $y_{\text{sink}} = 60$. This profile can be expressed as a solution of the one-dimensional diffusion equation with an instantaneous point source, given by

$$T(x) = T_0 + \frac{A_{\text{sink}}}{\sqrt{4\pi Dt}} \exp - \frac{(x-100)^2}{4Dt}, \tag{7}$$

where t is the time taken for the wave from the sink to the line at $y = 150$ and A_{sink} is an unknown parameter. A_{sink} is calculated by fitting the $T(x)$ profile with Eq. (7). For a given D, A_{sink} has very little variation with y_{sink}. In our simulation the maximum difference in A_{sink} due to sinks placed at different location was less than 4% of the mean A_{sink}.

In Figs. 7(a) and 7(c) we plot A_{sink} as a function of D for two and three dimensions, respectively. We assume that A_{sink} varies as aD^b, and we determine a and b from a linear regression analysis of a log-log plot. In two dimensions, $a = 0.37$ and $b = 0.27$ ($\mathscr{R} = 0.993$) and in three dimensions $a = 0.0079$ and $b = 0.52$ ($\mathscr{R} = 0.998$). In Figs. 7(b) and 7(c) we plot $A_{\text{sink}} = aD^b$ along with the numerically computed values in two and three dimensions, respectively.

The profile of arrival times shown in Fig. 7(a) suggests that diffusion processes in the medium play a critical role in the interaction of the sink with the propagating wave. When the sink interacts with the wave, it causes a perturbation proportional to A_{sink}, which then diffuses along the wave front. A_{sink} itself is determined by the diffusive processes that mediate the interaction between the wave front and the sink. In the next section, we develop a model of the interaction of the wave front with the sink in order to calculate the delay caused by a single sink.

B. Model of a single sink

To compute the effects of the sink, we adopt a frame of reference moving along with the wave front with the same velocity as the wave. We assume there is a sink at the origin ($x = 0$) and that the wave is traveling along the y direction in a medium of size $L_x \times L_y$. For our heuristic model, we assume that the effect of the sink can be modeled by passive diffusion of charge in a narrow segment of the medium of width (Δy).

During wave propagation in a homogeneous medium, the value of e in Eq. (1) at the maximum is $e = e_{\max}$. At the sink at $x = 0$, $e = e_{\text{sink}} = 0$. Associated with the potential $e(x,t)$ in the moving reference frame is a space-dependent charge, $q(x,t) = (\Delta y)Ce(x,t)$, where C is the capacitance per unit area and $q(x,t)$ is the charge per unit length. During wave propagation, the charge diffuses into the sink, leading to a change in the transmembrane potential along the wave front. We define the potential deficit along the wave front as $\mathscr{E}(x,t) = e_{\max} - e(x,t)$. When the wave front reaches the sink at time $t = 0$, $\mathscr{E}(x,t) = 0$ everywhere except in the neighborhood of a sink at $x = 0$, where $\mathscr{E}(x,t) = e_{\max}$.

The distribution of $\mathscr{E}(x,t)$ along the x direction can be calculated by solving the diffusion equation $\frac{\partial \mathscr{E}(x,t)}{\partial t} = D\frac{\partial^2 \mathscr{E}(x,t)}{\partial x^2}$ with the above initial condition. After a given time t, the distribution $\mathscr{E}(x,t)$ will be of the form [39]

$$\mathscr{E}(x,t) = e_{\max}\left[1 - \text{erf}\left(\frac{x}{2}\sqrt{\frac{1}{Dt}}\right)\right],$$

where $\text{erf}(u)$ is the error function. Therefore the average deficit in potential because of the sink along the wave front is [40]

$$\frac{1}{L_x}\int_0^\infty \mathscr{E}(x,t)\,dx = \frac{2e_{\max}}{L_x}\sqrt{\frac{Dt}{\pi}}. \tag{8}$$

Although the diffusion from the wave to the sink continues for the whole wavelength, once the wave front moves past the sink, the interaction of the rest of the wave with the sink will have minimal influence on the propagation. Hence t will be only a fraction of the time that the whole wave interacts with the sink. Although we cannot compute t exactly, we will assume that

$$t = \frac{\bar{r}}{v_0} = \frac{\bar{r}}{k}\sqrt{\frac{\tau}{D}}, \tag{9}$$

where $\bar{r}$ is the length of the wave front that interacts with the sink. We also assume that for relatively fast action potential upstroke, the wave front and hence $\bar{r}$ are independent of D, for the range of D we consider.

Because of this interaction, the sink would lead to delayed activation at points downstream from the sink. In order to compute the total delay T_d induced by the sink, we assume that there are active processes that lead to a depolarization at a rate $\dot{e}$. Consequently, from Eqs. (8) and (9), we find

$$T_d = \frac{2e_{\max}}{\dot{e}L_x}\sqrt[4]{\frac{\bar{r}^2 D\tau}{\pi^2 k^2}}, \tag{10}$$

where T_d is related to A_{sink} as $T_d = A_{\text{sink}}/L_x$ [Eq. (7)]. Hence Eq. (10) predicts A_{sink} to vary as $\sqrt[4]{D}$. This is consistent with our numerical simulations where A_{sink} varies as $D^{0.27}$ [Fig. 7(b)].

In order to extend this analysis to wave propagation past a single sink in three dimensions, we need to compute the potential deficit because of the sink. By using a similar argument to that used in two dimensions, the total change in potential in Eq. (8) would be proportional to $A_0 Dt$.

Consequently, the delay caused by a sink in three dimensions will be

$$T_d = k_3 \frac{e_{\max}}{\dot{e} L_x L_z} \frac{\sqrt{D\tau}\bar{r}}{k}, \tag{11}$$

i.e., A_{sink} varies as $\sqrt{D}$ in three dimensions, which is again consistent with what we find numerically where $A_{\text{sink}} \sim D^{0.52}$ [Fig. 7(c)].

This result enables us to compute the decrease in the observed velocity due to a single sink. For wave propagation over a distance L_y the velocity is

$$v = \frac{L_y}{T_0 + T_d}. \tag{12}$$

Now using Eq. (10) to calculate T_d, and assuming that $T_0 = L_y/v_0$ and $T_d \ll T_0$, we find

$$v = v_0 \left(1 - \frac{2e_{\max}}{L_x L_y \dot{q}} \sqrt[4]{\frac{k^2 \bar{r}^2 D^3}{\pi^2 \tau}}\right). \tag{13}$$

This equation for the conduction velocity slowing due to a single sink can be extended to describe the velocity slowing due to many sinks. Multiplying the delay caused by a single sink [Eq. (10)] by the number of sinks (n) we can obtain an expression for velocity in terms of ρ ($\rho = \frac{n}{L_x L_y}$), D, and other parameters:

$$v = v_0 \left(1 - \frac{k_2 e_{\max}}{\dot{e}} \sqrt[4]{\frac{\bar{r}^2}{\tau}} \rho D^{\frac{3}{4}}\right), \tag{14}$$

where k_2 is a dimensionless constant. Using $e_{\max}/\dot{e} \simeq \tau$ we can rewrite the above equation as

$$v = v_0 \left[1 - k_2 \rho \sqrt{\bar{r}} (D\tau)^{\frac{3}{4}}\right]; \tag{15}$$

i.e., the value of γ is 0.75. This is consistent with the numerically estimated value (0.77).

Similarly, we can obtain an expression for the velocity in a three-dimensional heterogeneous excitable media:

$$v = v_0 (1 - k_3 \rho \bar{r} D\tau), \tag{16}$$

where k_3 is a dimensionless constant in three dimensions. Here also the value of γ (1) is consistent with the numerically estimated value (1.02).

We have also verified that Eq. (15) applies even when sinks are of size $4\delta x^2$ and $9\delta x^2$. With larger sinks the distance over which the wave front interacts with the sink ($\bar{r}$) also becomes larger. We find that $\bar{r}$ scales approximately linearly with the length of the sink.

Equations (15) and (16) are of the form $v = v_0(1 - k\rho l_s^d)$, where d is the spatial dimension and $l_s^d = \sqrt{D\tau}(\bar{r}D\tau)^{\frac{d-1}{2}}$ is the effective volume occupied by the sink. To show that our numerical results are consistent with this theoretical prediction, we replot the data in Fig. 4(a) but now with ρl_s^2 along the abscissa and $v/\sqrt{\frac{D}{\tau}}$ along the ordinate [Fig. 8(a)]. Similarly, for the three-dimensional FHN model [Fig. 4(b)], we replot the same data with ρl_s^3 along the abscissa and $v/\sqrt{\frac{D}{\tau}}$ along the ordinate [Fig. 8(b)]. Here l_s is calculated using

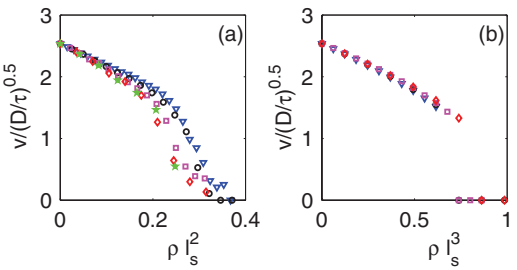

FIG. 8. (Color online) (a) The data plotted in Fig. 4(a) replotted with ρl_s^2 along the abscissa and $v/\sqrt{\frac{D}{\tau}}$ along the ordinate. Symbols (dots, circles, etc.) stand for velocity measured for $D = 0.5$ to 5.0 cm^2/s as in Fig. 4(a). (b) The data plotted in Fig. 4(b) replotted with ρl_s^3 along the abscissa and the ordinate as in (a). Symbols have the same meaning as in Fig. 4(b).

$\bar{r} = 0.02$ cm. With this rescaling, the data for different values of D line up together. Conduction fails in the two-dimensional medium when $\rho l_s^2 \sim 0.4$ and in the three-dimensional medium when $\rho l_s^3 \sim 0.7$.

V. DISCUSSION

In this paper we have studied the propagation of excitation waves in heterogeneous excitable media and the proposed relationships that relate the decrease of the conduction velocity to the proportion of randomly dispersed heterogeneities in the medium. Our results agree with several earlier numerical simulations in which a linear decrease in conduction velocity and subsequent wave breaks and conduction failure in both simple and more complex models of excitable media were noted [9,10,28,29,31]. In addition to this earlier work, we consider the effects of heterogeneities in a simple cellular automata model of excitable media, as well as using a nonlinear differential equation. We also compare the effects of two different types of heterogeneities of relevance to cardiac tissue: breaks and sinks.

The cellular automata model, in spite of its simplicity, is able to capture the essential properties of wave propagation seen in partial differential equation models. We can make analytic estimates of the dependence of the velocity of propagation on the model parameters. By equating the linear terms for the decrease of the conduction velocity with heterogeneity density for the cellular automata model in Eq. (4) and in Eq. (6) we obtain an estimate of the slope in the partial differential equation models of $k = 2\theta/(1 - \theta)$. From the value of k in Fig. 8(a) the corresponding θ in the FHN equations would be 0.45.

For sinks and breaks in the differential equation models, our main results are contained in Eqs. (6), (15) and (16), in which numerical results and theoretical arguments are used to extract the form of the dependence between conduction velocity and heterogeneities. With breaks, the slope of the velocity against ϕ is independent of D and τ, as predicted by Alonso *et al.* [9,10]. Alonso *et al.* further suggest that for breaks the velocity decrease is well described by the relationship

$$v = v_0 \sqrt{1 - \phi/\phi_c}, \tag{17}$$

where ϕ_c is the critical density at which propagation fails. Equating the first-order term from Eq. (17) with Eq. (6), we find

$$\phi_c = 1/(2c). \tag{18}$$

For the FHN equations, this gives agreement with the observed densities for propagation failure to within 10%. The propagation fails at the percolation threshold, in accordance with earlier studies [9,10]. While this is of theoretical interest, it may be less relevant to cardiac tissue where $\phi < \phi_c$ even in cases of extreme diffuse fibrosis [29].

One interesting question is whether there is a parameter that can predict the regimes of wave breaking, reentry, or conduction failure in a given excitable media. For both sinks and breaks the velocity changes as $v = v_0(1 - k\rho l^d)$, where l^d is the effective volume of the heterogeneity. For breaks $l^d = l_b^d$, the physical volume of the break. For sinks, $l^d = \sqrt{D\tau}(\bar{r}D\tau)^{\frac{d-1}{2}}$. The parameter ρl^d acts as such a dimensionless number. Further studies are required to test the generality of this result. Similarly, Eqs. (15) and (16) enable us to make predictions concerning the dependence of critical densities for propagation failure on D in media with sink heterogeneities. It has also been observed that the wave properties change near the boundaries of such heterogeneities [41]. We have ignored such spatial variations in wave properties and have expressed our results in terms of wave properties in the homogeneous media.

In the intact heart, structural abnormalities are often associated with an increased risk of serious and in some cases potentially fatal cardiac rhythms. In recent years, experimental observations have manipulated the degree of heterogeneities and the strength of coupling between cells in cardiac tissue using a variety of techniques including drugs that impair conduction between cells [13,14], growing mixtures of cells of different types [15], and inducing the growth of fibrous tissue, which has different conduction and coupling properties from normal cardiac muscle tissue [16,17]. Our results in the current paper are consistent with the general observation that decreased coupling between excitable cells and increased heterogeneity of cardiac tissue facilitates the initiation of blocked conduction and reentrant spiral waves. There is a need to combine theoretical analysis of heterogeneous excitable systems with experimental manipulation of heterogeneity and conduction to enable the development of methods to reduce the incidence of serious arrhythmias in the heart.

ACKNOWLEDGMENTS

We thank NSERC, MITACS, and the Quebec Heart and Stroke Foundation for financial support and Michael Guevara for helpful discussions. We also thank the anonymous referees for their comments and suggestions.

[1] A. Ishimaru, *Wave Propagation in Random Media* (Wiley, New York, 1997).
[2] J. Xin, *An Introduction to Fronts in Random Media* (Springer, New York, 2009).
[3] A. Winfree, J. Theor. Biol. **138**, 353 (1989).
[4] A. Panfilov, Chaos **8**, 57 (1998).
[5] F. H. Fenton, E. M. Cherry, H. M. Hastings, and S. J. Evans, Chaos **12**, 852 (2002).
[6] V. K. Vanag and I. R. Epstein, Science **294**, 835 (2001).
[7] V. K. Vanag and I. R. Epstein, Phys. Rev. Lett. **90**, 098301 (2003).
[8] O. Steinbock, P. Kettunen, and K. Showalter, Science **269**, 1857 (1995).
[9] S. Alonso, M. Bär, and R. Kapral, J. Chem. Phys. **131**, 214102 (2009).
[10] S. Alonso, R. Kapral, and M. Bär, Phys. Rev. Lett. **102**, 238302 (2009).
[11] M. Bär, E. Meron, and C. Utzny, Chaos **204**, 204 (2002).
[12] G. Bub, L. Glass, N. Publicover, and A. Shrier, Proc. Natl. Acad. Sci. USA **95**, 10283 (1998).
[13] G. Bub, A. Shrier, and L. Glass, Phys. Rev. Lett. **88**, 058101 (2002).
[14] G. Bub, A. Shrier, and L. Glass, Phys. Rev. Lett. **94**, 28105 (2005).
[15] S. Zlochiver, V. Munoz, K. L. Vikstrom, S. M. Taffet, O. Berenfeld, and J. Jalife, Biophys. J. **95**, 4469 (2008).
[16] B. Burstein, P. Comtois, G. Michael, K. Nishida, L. Villeneuve, Y. Yeh, and S. Nattel, Circ. Res. **105**, 1213 (2009).
[17] K. Tanaka *et al.*, Circ. Res. **101**, 839 (2007).
[18] Z. Y. Lim, B. Maskara, F. Aguel, R. Emokpae, and L. Tung, Circulation **114**, 2113 (2006).
[19] D. Li, S. Fareh, T. K. Leung, and S. Nattel, Circulation **100**, 87 (1999).
[20] A. Pumir, V. Nikolski, M. Hörning, A. Isomura, K. Agladze, K. Yoshikawa, R. Gilmour, E. Bodenschatz, and V. Krinsky, Phys. Rev. Lett. **99**, 208101 (2007).
[21] F. Xie, Z. Qu, and A. Garfinkel, Phys. Rev. E **58**, 6355 (1998).
[22] F. Xie, Z. Qu, J. N. Weiss, and A. Garfinkel, Phys. Rev. E **63**, 031905 (2001).
[23] T. K. Shajahan, S. Sinha, and R. Pandit, Phys. Rev. E **75**, 011929 (2007).
[24] T. K. Shajahan, A. R. Naik, and R. Pandit, PLoS ONE **4**, e4738 (2009).
[25] J. M. Starobin and C. F. Starmer, Phys. Rev. E **54**, 430 (1996).
[26] K. H. W. J. ten Tusscher and A. V. Panfilov, Am. J. Physiol. Heart Circ. Physiol. **284**, H542 (2003).
[27] K. H. W. J. ten Tusscher and A. V. Panfilov, Multiscale Model. Simul. **3**, 265 (2005).
[28] B. E. Steinberg, L. Glass, A. Shrier, and G. Bub, Philos. Trans. R. Soc. London Ser. A **364**, 1299 (2006).
[29] K. H. W. J. ten Tusscher and A. Panfilov, Europace **9**, vi38 (2007).
[30] J. M. Greenberg and S. P. Hastings, SIAM J. Appl. Math. **34**, 515 (1978).
[31] K. H. W. J. ten Tusscher and A. V. Panfilov, Phys. Rev. E **68**, 062902 (2003).

[32] K. Showalter and J. J. Tyson, J. Chem. Educ. **64**, 742 (1987).
[33] A. T. Winfree, *1992 Lectures in Complex Systems*, Vol. 5, Chap. The Geometry of Excitability (Addison-Wesley, Reading, MA, 1993), pp. 207–298.
[34] D. Stauffer and A. Aharony, *Introduction to Percolation Theory* (Taylor & Francis, London, 1992).
[35] M. E. J. Newman and R. M. Ziff, Phys. Rev. Lett. **85**, 4104 (2000).
[36] M. J. Lee, Phys. Rev. E **78**, 031131 (2008).
[37] I. Sendiña-Nadal, V. Pèrez-Muñuzuri, M. Gòmez-Gesteira, A. P. Muñuzuri, and V. Pèrez-Villar, Int. J. Bifurcation Chaos **12**, 2353 (1999).
[38] V. S. Zykov, Biophysics **25**, 906 (1980).
[39] J. Mathews and R. L. Walker, *Mathematical Methods of Physics* (Benjamin, New York, 1964).
[40] WolframAlpha, http://www.wolframalpha.com/input/?i=Integrate[Erfc[a*x]%2C x%2C0%2CInfinity] [accessed 3 June 2011].
[41] J. W. Cain and D. G. Schaeffer, Math. Med. Biol. **25**, 21 (2008).